Proceedings of the 11th Brazilian Congress of Thermal Sciences and Engineering -- ENCIT 2006
Braz. Soc. of Mechanical Sciences and Engineering -- ABCM, Curitiba, Brazil, Dec.5-8, 2006

Paper CIT06-0247

THE EFFECTS OF INTERFERENCE BETWEEN TWO CIRCULAR CYLINDERS ARRANGED IN TANDEM BY VORTEX METHOD USING TURBULENCE MODELING

Luiz Antonio Alcântara Pereira
Instituto de Engenharia Mecânica, UNIFEI, CP 50, Itajubá, Minas Gerais, 37500-903, Brasil
e-mail: luizantp@unifei.edu.br

Miguel Hiroo Hirata
FAT/UERJ
Campus Regional de Resende
Estrada Resende - Riachuelo, Resende, RJ
e-mail: hirata@fat.uerj.br

Abstract. *The work presents an investigation of the aerodynamics characteristics of two circular cylinders in a tandem arrangement for various values for the gap between the cylinders at high Reynolds number using the viscous vortex element method. The Vortex Method is also modified to take into account the sub grid-scale phenomena; a second-order velocity structure function model is adapted to the Lagrangian scheme. The dynamics of the wakes is computed using the convection-diffusion splitting algorithm, where the convection process is carried out with a Lagrangian second-order Adams-Bashforth time-marching scheme, and the diffusion process is simulated using the random walk scheme. The aerodynamics forces and pressure distributions acting on two circular cylinders are computed using the integral derived from the pressure Poisson equation; comparisons are made with experimental results available in the literature.*

Keywords: *vortex method, panels methods, tandem arrangement, turbulence model, aerodynamics loads.*

1. Introduction

Flow behavior around circular cylinders have been investigated by numerous researches in the past few decades. In many cases of engineering practices, objects often appear in the form of groups of cylinders of circular shape, e.g. tube banks of compact heat exchangers, cable bundlers, supports of off-shore platform, etc. Due the mutual interference between cylinders at close proximity, the aerodynamics characteristics, such as fluctuating lift and drag forces, vortex-shedding patterns and fluctuating pressure distributions, for each member of a group are completely different from isolated ones. When a cylinder is placed in the wake of another in cross-flow, the so-called tandem arrangement, its unsteady loading becomes dependent not only on the flow activities in its wake, but also on those in the wake of the upstream cylinder.

Numerous investigations have been made of the flow past two circular cylinders, which is the simplest case of a group, in the last three decades. Zdravkovich (1977) and Ohya *et al.* (1989) presented an extensive review of the state of knowledge of flow across two cylinders in various arrangements. Previous investigations of tandem configurations by Biermann and Herrnstein (1933), Kostic and Oka (1972), Novak (1974), Zdravkovich and Pridden (1975, 1977), Okajima (1979), Igarashi (1981, 1984), Hiwada *et al.* (1982), Arie *et al.* (1983), Jendrzejczyk and Chen (1986) have revealed considerable complexity in fluid dynamics as the spacing or gap between the cylinders is changed.

The interference phenomena are highly non-linear and there are many discrepant points in previous works. Arie *et al.* (1983) pointed out that fluctuation in drag force acting both cylinders is weakly dependent on spacing. On the other hand, Igarashi (1981) reported that the fluctuation in pressure associated with fluctuation in aerodynamics forces (lift and drag) acting on a downstream cylinder is strongly dependent on gap between the cylinders.

Recently, the Vortex Method was employed by Teixeira da Silveira *et al.* (2005) to simulate the vortex-shedding flow from two tandem cylinders in cross-flow; the aerodynamic characteristics are investigated at a Reynolds number of 6.5×10^4 and comparisons are made with experimental results presented by Alam *et al.* (2003). As the simulations showed, the numerical results obtained are in overall good agreement with the experimental results used for comparison, especially in the simulations for the upstream cylinder. Some discrepancies observed in the determination of the aerodynamics loads for the downstream cylinder may be attributed to errors in the treatment of vortex element moving away from a solid surface. Because every vortex element has different strength of vorticity, it will diffuse to different location in the flow field. It seems impossible that every vortex element will move to same ε-layer normal to the solid surface. In the present method all nascent vortices were placed into the cloud through a same displacement normal to the panels.

The Vortex Method have been developed and applied for analysis of complex, unsteady and vortical flows in relation to problems in a wide range of industries, because they consist of simple algorithm based on physics of flow (Kamemoto, 2004). Vortex cloud modeling offers great potential for numerical analysis of important problems in fluid

mechanics. A cloud of free vortices is used in order to simulate the vorticity, which is generated on the body surface and develops into the boundary layer and the viscous wake. Each individual free vortex of the cloud is followed during the numerical simulation in a typical Lagrangian scheme. This is in essence the foundations of the Vortex Method (Chorin, 1973; Sarpakaya, 1989; Sethian, 1991; Lewis, 1999, Kamemoto, 2004 and Alcântara Pereira *et al.*, 2004, 2005).

Vortex Method offers a number of advantages over the more traditional Eulerian schemes: (a) the absence of a mesh avoids stability problems of explicit schemes and mesh refinement problems in regions of high rates of strain; (b) the Lagrangian description eliminates the need to explicitly treat convective derivatives; (c) all the calculation is restricted to the rotational flow regions and no explicit choice of the outer boundaries is needed a priori; (d) no boundary condition is required at the downstream end of the flow domain.

For the grid methods, such as finite difference method and finite element method, the governing Navier-Stokes equations are solved directly. However, the flows around cylinder arrays are usually computed at Reynolds number (Re) up to a few hundred (Fornberg, 1985 and Jackson, 1987) while the Re for flows around cylinders in many engineering applications is of much higher order O (10^6). In such circumstance, the traditional Eulerian schemes will not give a satisfactory prediction within a reasonable computational cost. Also, the pre-processing and mesh-generation are time-consuming for the grid method in numerical simulations.

The development of Lagrangian LES models for Vortex Method has been discussed in the literature. Chorin (1993a, 1993b) presented the hairpin-removal schemes, which combine a filament-based method with a local mesh redistribution algorithm that removes the filaments small scales or "hairpin"; these schemes have been used in various applications, including boundary layers (Bernard, 1996), vortex breakdown (Saghbine, 1996) and vortex reconnection (Fernandez *et al.,* 1996). In their simplest form, hairpin-removal schemes rely on the redistribution scheme to filter out the small scales but maintain the same governing equation for the large scales. Thus the effect of the unresolved scales is assumed to be accounted for by the hairpin removal process. The dynamic eddy diffusivity model is not incorporated into a 3D Lagrangian particle scheme. The effect of the sub filter scale (SFS) vorticity stresses on the motion of the resolved scales is not accounted for.

Leonard and Chua (1989) applied the Smagorinsky model in simulations of three-dimensional interaction between interlocked vortex rings and interaction between two colliding vortex rings; a nonlinear core-spreading algorithm was used analogous to the Smagorinsky sub grid scale viscosity used in large eddy simulation. Viscous effects must be included to prevent the physical divergence of the inviscid equations.

A dynamic eddy viscosity model of sub filter scale (SFS) of vorticity stresses was presented by Mansfield *et al.* (1998, 1999); in this model, a Lagrangian particle method was applied in the simulation of collision of coaxial vortex rings. The scheme combines 3D, adaptive, viscous, vortex element method with a dynamic eddy viscosity model of sub filter scale. In addition, it is shown that the Lagrangian LES scheme captures several experimentally observed features of the ring collisions, including turbulent breakdown into small-scale structures and the generation of small-scale radially propagating vortex rings. The computations indicated that the model has some weaknesses, as the simplified nature of the removal process, which is presently based on merging particles lying within a critical cut-off period. Another area where additional work is needed is in clearly quantifying the effect of the SFS model, and distinguishing it from the effect of the removal scheme.

Cotte *et al.* (2002) investigated reliability of numerical analysis of turbulent structures using a vortex-in-cell method presenting a comparison of the performance of the Vortex Method and the spectral method in a homogeneous turbulent flow at low Reynolds number and a vortex reconnection case at a moderate Reynolds number.

Alcântara Pereira *et al.* (2002) proposed a local second-order velocity structure function to take into account the micro scale manifestations of the turbulence and applied it into simulation of vortex shedding flow about a circular cylinder by a Vortex Method.

In the present paper, the Vortex Method is employed to simulate the vortex-shedding flow from two tandem cylinders in cross-flow; the turbulence modeling is taking into account using a second-order velocity structure function model (Alcântara Pereira *et al.*, 2002). The aerodynamic characteristics are investigated at a Reynolds number of 6.5×10^4 and comparisons are made with experimental results presented by Alam *et al.* (2003).

2. Formulation of the Physical Problem

Consider the incompressible fluid flow of a Newtonian fluid around two circular cylinders in a tandem arrangement an unbounded two-dimensional region. Figure 1 shows the incident flow, defined by free stream speed U and the domain Ω with boundary $S = S_1 \cup S_2 \cup S_3$, S_1 being the upstream cylinder surface, S_2 being the downstream cylinder surface and S_3 the far away boundary.

The viscous and incompressible fluid flow is governed by the continuity and the Navier-Stokes equations, which can be written in the form (Alcântara Pereira *et al.*, 2002)

$$\frac{\partial \overline{w_i}}{\partial x_i} = 0 \tag{1}$$

$$\frac{\partial \overline{w_i}}{\partial t} + \overline{w_j}\frac{\partial \overline{w_i}}{\partial x_j} = -\frac{1}{\rho}\frac{\partial \bar{p}}{\partial x_i} + 2\frac{\partial}{\partial x_j}\left[(\upsilon + \upsilon_t)\overline{S_{ij}}\right], \tag{2}$$

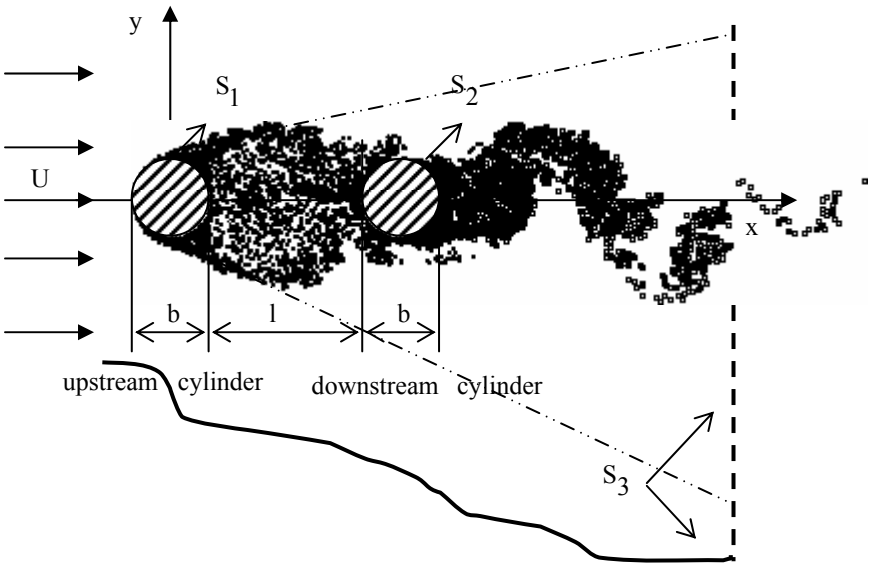

Figure 1. Flow around two circular cylinders in a tandem arrangement.

where the summation convention applies. The above governing equations were filtered ($w_i = \overline{w_i} + w_i'$, w_i' denotes the fluctuation field), υ is the fluid kinematics viscosity coefficient, υ_t is the eddy viscosity coefficient, ρ is the fluid density, $\overline{S_{ij}}$ is the deformation tensor of the filtered field and p is the pressure.

The large structures are governed by Eq. (2) and the eddy-viscosity assumption (Boussinesq's hypothesis) is used to model the sub grid scale tensor $T_{ij} = -2\upsilon_t \overline{S_{ij}}$ (Smagorinsky, 1963).

For a complete definition of the problem the impermeability and no-slip conditions on the two circular cylinders surface are written as

$$w_n = \mathbf{w} \cdot \mathbf{e}_n = 0 \tag{3}$$

$$w_\tau = \mathbf{w} \cdot \mathbf{e}_\tau = 0 \tag{4}$$

where $\mathbf{e}_n$, $\mathbf{e}_\tau$ and $\mathbf{w}$ are unit normal vector, unit tangential vector and velocity vector, respectively. One assumes that, far away, the perturbation caused by the circular cylinders arranged in tandem fades away as

$$|\mathbf{w}| \to 1 \text{ at } S_3 . \tag{5}$$

In order to take into account the local activity of turbulence, Métais and Lesieur (1992) considered that the small scales may not be too far from isotropy and proposed to use the local kinetic-energy spectrum $E_{(k_c)}$ at the cut-off wave number (k_c) to define the eddy viscosity υ_t. Using a relation proposed by Batchelor (1967) the local spectrum at k_c is calculated with a local second-order velocity structure function $\overline{F_2}$ of the filtered field Lesieur and Métais (1996)

$$\overline{F_2}(\mathbf{x},\Delta,t)=\overline{\left\|\overline{\mathbf{w}}(\mathbf{x},t)-\overline{\mathbf{w}}(\mathbf{x}+\mathbf{r},t)\right\|^2}\Big|_{\|\mathbf{r}\|=\Delta}. \tag{6}$$

From the Kolmogorov spectrum the eddy viscosity can be written as a function of $\overline{F_2}$

$$\upsilon_t(\mathbf{x},\Delta,t)=0.105C_k^{-\frac{3}{2}}\Delta\sqrt{\overline{F_2}(\mathbf{x},\Delta,t)}, \tag{7}$$

where $C_k=1.4$ is the Kolmogorov constant. The great computational advantage of this formulation over the Smagorinsky (1963) model is that in Eq. (6) the notion of velocity fluctuations (differences of velocity) is used instead of the rate of deformation (derivatives). The velocities $\overline{\mathbf{w}}(\mathbf{x}+\mathbf{r})$ are calculated over the surface of a sphere of radius Δ.

Alcântara Pereira *et al* (2002) adapted the definition of the second-order velocity structure function $\overline{F_2}$ to the Lagrangian scheme in 2-D as

$$\overline{F_2}=\frac{1}{NV}\sum_{l=1}^{NV}\left\|\mathbf{w}(\mathbf{x})-\mathbf{w}(\mathbf{x}+\mathbf{r}_l)\right\|_l^2\left(\frac{\sigma_{0\upsilon_t}}{\|\mathbf{r}_l\|}\right)^{\frac{2}{3}}. \tag{8}$$

In Eq. (8), NV is the number of discrete vortices of the cloud found in the region defined by the distances $r_1=0.1\sigma_{0\upsilon_t}$ and $r_2=(1.0+f_2)\sigma_{0\upsilon_t}$ from the centre of the reference vortex, where $\sigma_{0\upsilon_t}$ is the core radius of a Lamb vortex, see Eq. (16), which is used as a model for the discrete vortices of the cloud. A correction $\left(\sigma_{0\upsilon_t}/\|\mathbf{r}_l\|\right)^{2/3}$ is necessary due to the fact that the NV vortices are not located at equal distance from the centre of the reference vortex.

$\overline{F_2}$ represents a local statistical average of square velocity differences between free vortices located in the region defined by the distances $r_1=0.1\sigma_{0\upsilon_t}$ and $r_2=(1.0+f_2)\sigma_{0\upsilon_t}$ from the centre of the reference vortex. Physically, this function represents the flow fluctuation (turbulent activities) in the neighbourhood of the vortex located at **x.**

Defining the Reynolds number as

$$Re=\frac{bU}{\upsilon}, \tag{9}$$

where U and b are representative quantities, the dynamics of the fluid motion, governed by the boundary-value problem (1)-(5), can be alternatively studied by taking the curl of Eq. (2), obtaining the new 2-D vorticity transport equation

$$\frac{\partial\omega}{\partial t}+\mathbf{w}\cdot\nabla\omega=\frac{1+\upsilon_t^*}{Re}\nabla^2\omega, \tag{10}$$

in which ω is the only non-zero component of the vorticity vector and

$$\upsilon_t^*=\frac{\upsilon_t}{\upsilon}. \tag{11}$$

It is also worth to observe that the turbulence is essentially a 3-D phenomenon and yet one is modelling it using a 2-D approach; obviously it is then assumed 2-D turbulence. With this procedure one are still left with important turbulence aspects and the final results are also improved. The use of 2-D turbulence may explain some numerical results that depart from the experimental values.

3. Numerical method

According to the viscous splitting algorithm (Chorin, 1973) convection and the diffusion of vorticity can be handled independently for each time increment. Thus the vorticity convection is governed by

$$\frac{\partial \omega}{\partial t} + \mathbf{w} \cdot \nabla \omega = 0 \tag{12}$$

and diffusion of vorticity by

$$\frac{\partial \omega}{\partial t} = \frac{1 + \upsilon_t^*}{\mathrm{Re}} \nabla^2 \omega \,. \tag{13}$$

3.1 Discrete vortex method (large scale simulation)

In a physical sense vorticity is generated on the circular cylinders surface so as to satisfy the no-slip condition, Eq. (4). The discrete vortex method represents the vorticity by discrete vortices, whose transport at each time increment is carried out in sequence. Convection is governed by Eq. (12) and the velocity field is given by

$$u - iv = 1 + \frac{i}{2\pi} \sum_{n=1}^{2M} \gamma(S_n) \int_{\Delta S_n} \frac{d}{dz} \ln(z - \zeta) d\zeta + \frac{i}{2\pi} \sum_{k=1}^{N} \frac{\Delta \Gamma_k}{z - z_k} \,. \tag{14}$$

Here, u and v are the x and y components of the velocity vector $\mathbf{w}$ and $i = \sqrt{-1}$. The first term in the right hand side is the contribution of the incident flow; the summation of $2M$ integral terms comes from the panels distributed on the two circular cylinders surface. The second summation is associated to the velocity induced by the cloud of N free vortices; it represents the vortex-vortex interaction.

In this paper, an improvement was also introduced in the convective step of the simulation; by using the anti symmetry property of the vortex-vortex velocity induction, the computational effort was reduced; this is an important feature, since the vortex-vortex velocity induction calculation is the most time consuming part of the simulation.

In order to remove the singularity in the second summation of Eq. (14) Lamb vortices are used, whose mathematical expression for the induced velocity of the kth vortex with strength $\Delta\Gamma_k$ in the circumferential direction u_{θ_k}, is (Mustto *et al.*, 1998)

$$u_{\theta_k} = \frac{\Delta \Gamma_k}{2\pi r} \left\{ 1 - \exp\left[-5.02572 \left(-\frac{r}{\sigma_0} \right)^2 \right] \right\} \tag{15}$$

In this particular equation r is the radial distance between the vortex center and the point in the flow field where the induced velocity is calculated. The radius of the Lamb vortex core σ_0, is modified to (Alcântara Pereira *et al.*, 2002)

$$\sigma_{0_{\upsilon_t}} = 4.48364 \sqrt{\frac{\Delta t \left(1 + \upsilon_t^* \right)}{\mathrm{Re}}} \,. \tag{16}$$

Each Lamb discrete vortex distributed in the flow field is followed during numerical simulation according to the Adams-Bashforth second-order formula (Ferziger, 1981)

$$\mathbf{r}(t + \Delta t) = \mathbf{r}(t) + \left[1.5\mathbf{w}(t) - 0.5\mathbf{w}(t - \Delta t) \right] \Delta t + \xi \tag{17}$$

in which $\mathbf{r}$ is position of a fluid particle, Δt is the time increment and ξ is the random walk, representing diffusion of vorticity (Lewis, 1991). This displacement is modified to (Alcântara Pereira *et al.*, 2002)

$$\xi = \sqrt{\frac{4\Delta t \left(1 + \upsilon_t^* \right)}{\mathrm{Re}} \ln\left(\frac{1}{p} \right)} \left[\cos(2\pi Q) + i \sin(2\pi Q) \right] \tag{18}$$

P and Q are random numbers between 0.0 and 1.0.

The pressure calculation starts with the Bernoulli function, defined by Uhlman (1992) as

$$Y = p + \frac{w^2}{2},\ w = |\mathbf{w}| \tag{19}$$

Kamemoto (1993) used the same function and starting from the Navier-Stokes equations was able to write a Poisson equation for the pressure. This equation was solved using a finite difference scheme. Here the same Poisson equation was derived and its solution was obtained through the following integral formulation (Shintani and Akamatsu, 1994)

$$H\overline{Y_i} - \int_{S_1} \overline{Y}\nabla G_i \cdot \mathbf{e}_n \, dS = \iint_{\Omega} \nabla G_i \cdot (\mathbf{w} \times \boldsymbol{\omega}) d\Omega - \frac{1}{Re}\int_{S_1} (\nabla G_i \times \boldsymbol{\omega}) \cdot \mathbf{e}_n \, dS \tag{20}$$

where H is 1.0 inside the flow (at domain Ω) and is 0.5 on the boundaries S_1 and S_2. $G_i = (1/2\pi)\log R^{-1}$ is the fundamental solution of Laplace equation, R being the distance from i^{th} vortex element to the field point.

It is worth to observe that this formulation is specially suited for a Lagrangian scheme because it utilizes the velocity and vorticity field defined at the position of the vortices in the cloud. Therefore it does not require any additional calculation at mesh points. Numerically, Eq. (20) is solved by mean of a set of simultaneous equations for pressure Y_i. The pressure coefficient on a panel control point i is calculated according to $C_{p_i} = 1 + Y_i$.

3.2 Turbulence modeling (micro scale simulation)

The concept of eddy viscosity, υ_t, as defined by Eq. (7), has to be considered in order to take into consideration the micro scale manifestations of the turbulence.

In the numerical simulation, consider a point vortex of the cloud, which is located at point L. The value of the velocity structure function $\overline{F_2}$, which measures the turbulence manifestations, is statistically sound only if the neighbourhood of L is sufficiently populated with other point vortices. After some numerical experiments with the flow around two circular cylinders arranged in tandem, it was assumed that this happens if $(NV/A) \geq 5000$, where NV is the number of point vortices in the region, of area A, defined by two circumferences centred in L and with radius $r_1 = 0.1\sigma_{0_{\upsilon_t}}$ and $r_2 = 1.5\sigma_{0_{\upsilon_t}}$.

It is important to observe that the viscous diffusion of vorticity was taken care of by using the random walk method, a molecular (laminar) diffusion process. In our approach the variation of the core radius is only performed locally where the flow is turbulent, that means an additional (turbulent) diffusion process.

4. Results and discussion

Table 1 presents all cases studied for two circular cylinders in a tandem arrangement at a subcritical Reynolds number of 6.5×10^4 without turbulence modeling (Teixeira da Silveira *et al.*, 2005). In the calculations, each cylinders surface was represented by fifty (M=50) straight-line vortex panels with constant density. All runs were performed with 600 time steps of magnitude $\Delta t=0.05$. The time increment was evaluated according to $\Delta t = 2\pi k/M$, $0 < k \leq 1$ (Mustto *et al.*, 1998). In each time step the nascent vortices were placed into the cloud through a displacement $\varepsilon = \sigma_0 = 0.03b$ normal to the panels. The aerodynamics forces and pressure distributions computations starts at t=15. The aerodynamics force coefficients are calculated through the integration of the pressure coefficient distribution on the each cylinders surface.

Table 1. Comparison of the mean drag coefficient with experimental results without turbulence modeling, for $Re=6.5 \times 10^4$.

Case	l/b	Upstream cylinder		Downstream cylinder	
		C_D^+	$\overline{C_D^*}$	C_D^+	$\overline{C_D^*}$
I	0.1	1.0953	1.1500	-0.5697	-0.5447
II	0.5	---	0.9866	-0.3884	-0.2997
III	1.0	1.0531	1.3664	-0.2366	0.1130
IV	2.0	0.9866	1.3434	-0.1345	0.3652
V	3.5	1.2612	1.3677	0.2766	0.4613
VI	4.0	1.2319	1.4174	0.2661	0.3015
VII	8.0	1.2040	1.4324	0.3604	0.8693

$^+$ Experimental results (Alam *et al.*, 2003) * Present calculation without turbulence modeling

Within the results presented in Table 1, is observed a disagreement of the numerical results to the experimental results (Alam *et al.*, 2003) of cases III, IV and VII on the time-averaged drag coefficient, C_D, of the downstream cylinder. The mean drag coefficients of the downstream cylinder are much higher than the experimental values and, therefore, do not reflect a good simulation of the flow. The differences encountered in the comparison of the numerical results with the experimental results are attributed mainly the inherent three-dimensionality of the real flow for such a value of the Reynolds number, which is not modeled in the present simulation. A purely two-dimensional computation of such flow must produce higher values for the drag coefficient, as obtained for our simulation.

No attempts to simulate the flow for M greater than 50 were made since the operation count of the algorithm is proportional to the square of N. As M increases N also tends to increase, and the computation becomes expensive.

Experiments (Alam *et al.*, 2003) were conducted in a low-speed, closed-circuit wind tunnel with a test section of 0.6 m height, 0.4 m width, and 5.4 m length. The level of turbulence in the working section was 0.19%. The cylinders used as test models were made of brass and were each 49 mm in diameter. The geometric blockage ratio and aspect ratio at the test section were 8.1% and 8.2, respectively. None of the results presented were corrected for the effects of wind-tunnel blockage.

As the simulations show, the numerical results obtained are in overall good agreement with the experimental results used for comparison, especially in the simulations for the upstream cylinder. Some discrepancies observed in the determination of the aerodynamics loads for the downstream cylinder for spacing l/b=1.0, l/b=2.0 and l/b=8.0 may be attributed to errors in the treatment of vortex element moving away from a solid surface. Because every vortex element has different strength of vorticity, it will diffuse to different location in the flow field. It seems impossible that every vortex element will move to same ε-layer normal to the solid surface. In the present method all nascent vortices were placed into the cloud through a displacement $\varepsilon = \sigma_0 = 0.03b$ normal to the panels.

The sub-grid turbulence modeling is of significant importance for the numerical simulation. The results of this analysis, taking into account the sub-grid turbulence modeling are presented in Table 2.

Table 2. Comparison of the mean drag coefficient with experimental results with turbulence modeling, for $Re=6.5 \times 10^4$.

Case	l/b	Upstream cylinder		Downstream cylinder	
		C_D^+	$\overline{C_D^*}$	C_D^+	$\overline{C_D^*}$
I	0.1	1.0953	0.8782	-0.5697	-0.9447
II	0.5	---	0.8751	-0.3884	-0.2225
III	1.0	1.0531	1.0607	-0.2366	0.1142
IV	2.0	0.9866	1.1687	-0.1345	0.5315
V	3.5	1.2612	1.2034	0.2766	0.3202
VI	4.0	1.2319	1.1551	0.2661	0.5609
VII	8.0	1.2040	1.1962	0.3604	0.5224

$^+$ Experimental results (Alam *et al.*, 2003) * Present calculation with turbulence modeling

As it can be seen, qualitatively, the behaviour of the results with sub-grid scale modeling is more regular, showing already the improvements obtained with turbulence modeling. The sub-grid scale modeling improved the results but the drag coefficient is still high especially for downstream cylinder for spacing l/b=1.0 and l/b=2.0.

More investigations are needed and one can imagine that with the use of more panels (and therefore more free vortices in the cloud) the results tend to be in closer agreement with the experiments.

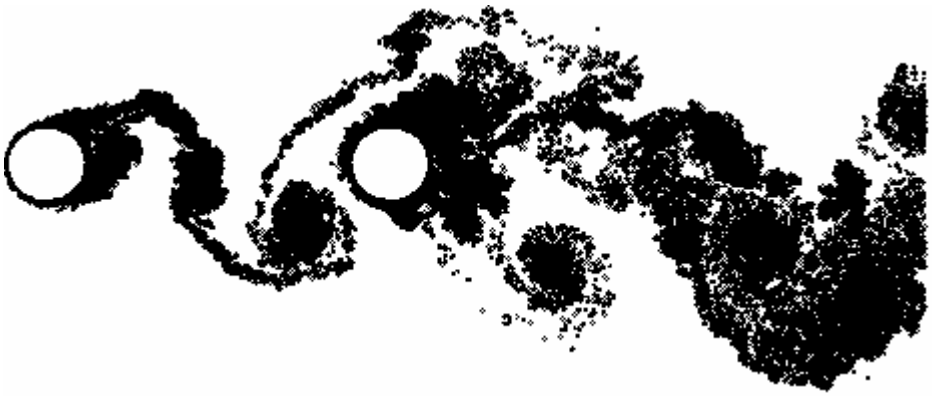

Figure 2. Position of the wakes vortices at t=60 for case VI; $Re=6.5 \times 10^4$, $\varepsilon = \sigma_0 = 0.03b$, $\Delta t=0.05$, M=50, l/b=4.0.

Figure 2 shows the position of the wake vortices for case VI using turbulence modeling at last step of the computation (t=60), where we can clearly observe the formation and shedding of large eddies in the wakes. This process occurs alternately on the upper and lower surfaces of each cylinder arranged in tandem. We can also visualize the vortex pairing process, where the vortices rotate in opposite directions and are connected to each other by a vortex sheet. The separation phenomenon associated with the existence of adverse pressure gradients on the surface of the upstream and downstream cylinders occurs alternately on the top and bottom surfaces.

Computed values for the distribution of the mean pressure coefficient along the cylinders surface is shown in Figure 3 for spacing l/b=3.5. Figure 3a shows the experimental results, which are compared with the ones obtained using the Vortex Method simulation without turbulence modeling, whereas in Fig. 3b the results of the Vortex Method refer to the simulation with turbulence modeling.

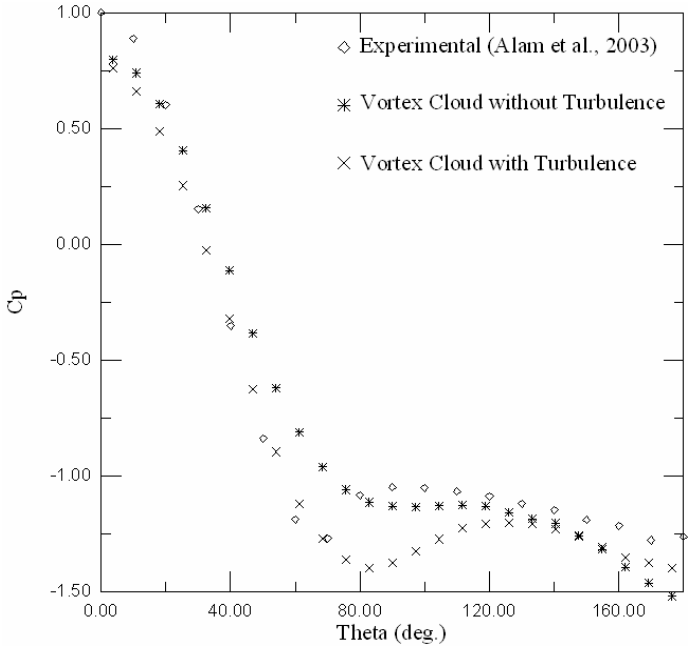

(a) Upstream cylinder (l/b=3.5)

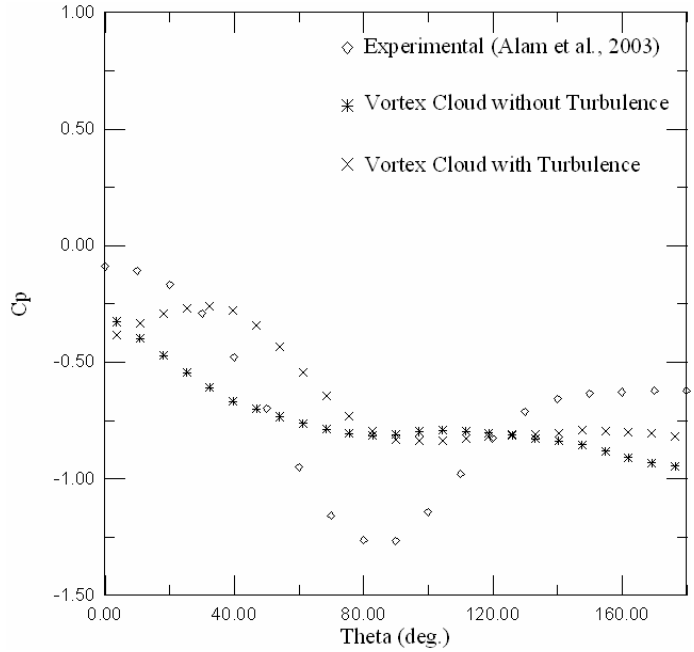

(b) Downstream cylinder (l/b=3.5)

Figure 3. Pressure distribution along the surface of the upstream and downstream cylinders, for $Re=6.5x10^4$.

The graph for the variation with time of the lift and drag coefficients with the sub grid scale modeling can be seen in Fig. 4 for spacing l/b=3.5. Figure 4b shows that the drag coefficient (C_D) for downstream cylinder oscillates around $\overline{C_D^*}$ = 0.3222; the mean value is very good when the sub-grid scale modeling is considered.

Finally the sub-grid turbulence modeling is of significant importance for the numerical simulation, especially for flow around bluff bodies (Alcântara Pereira *et al.,* 2002), and a necessary step for the roughness modeling, which is in preparation to be presented elsewhere.

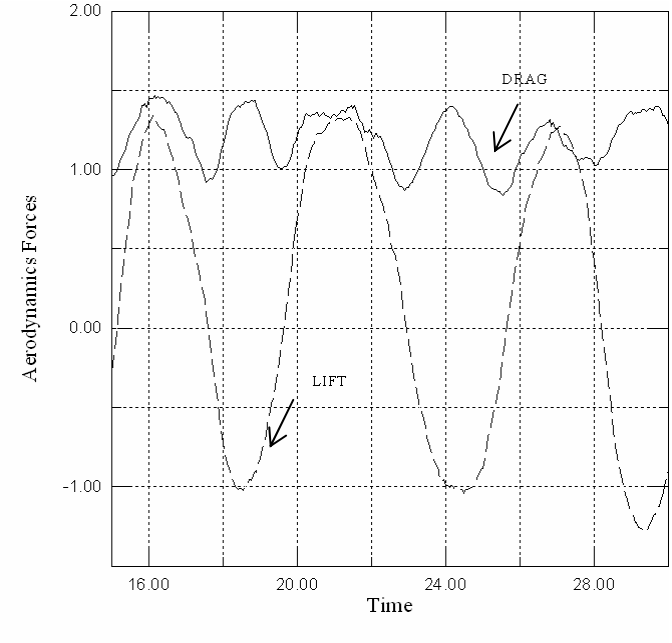

(a) Upstream cylinder (l/b=3.5)

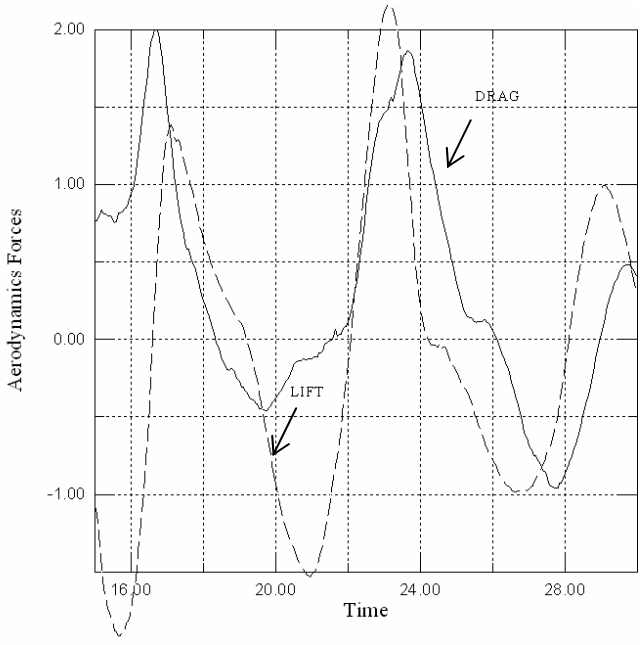

(b) Downstream cylinder (l/b=3.5)

Figure 4. Variation of C_D and C_L with time with turbulence modeling, Re=6.5x10^4, $\varepsilon = \sigma_0$ =0.03b, Δt=0.05, M=50.

5. Conclusions

The main objective of the work with the implementation and initial test of a sub-grid scale model in connection with the Vortex Method has been achieved. The results show that the Vortex Method with turbulence modeling, can improve previously obtained results without modeling, being therefore encouraging. Additional analysis of the

influence of numerical parameters will have to be carried out. The differences encountered in the comparison of the numerical results with the experimental results are attributed mainly to the inherent three-dimensionality of the real flow for such a value of the Reynolds number, which is not modelled in the simulation.

The use of a fast summation scheme to determine the vortex-induced velocity, such as the Multiple Expansion scheme, allows an increase in the number of vortices and a reduction of the time step, which increases the resolution of the simulation, in addition to a reduction of the CPU time, which allows a longer simulation time to be carried out. The present calculation required 18 h of CPU time in an Intel(R) Pentium(R) 4 CPU 1700 MHz.

Future work will investigate the variation in Strouhal number with increase in spacing l/b between two cylinders in a tandem arrangement.

Finally, despite the differences presented in this preliminary investigation, the results are promising, that encourages performing additional tests in order to explore the phenomena in more details.

6. Acknowledgement

The authors would like to acknowledge FAPEMIG (Proc. TEC-748/04) and CNPq for the financial support during the time of this project.

7. References

Alam, M. M., Moriya, M., Takai, K. and Sakamoto, 2003, "Fluctuating Fluid Forces Acting on Two Circular Cylinders in a Tandem Arrangement at a Subcritical Reynolds Number", J. Wind Eng. Ind Aerodyn., 91, pp. 139-154.

Alcantara Pereira, L.A., Ricci, J.E.R. and Hirata, M.H., 2005, "Simulation of Linear Cascade Vortex Cloud Interaction with Turbulence Modeling", Intern'l Society of CFD, Vol. 14, No. 2, July, pp. 1-10.

Alcântara Pereira, L.A., Hirata, M.H. and Manzanares Filho, N. 2004, "Wake and Aerodynamics Loads in Multiple Bodies - Application to Turbomachinery Blade Rows", J. Wind Eng. Ind Aerodyn., 92, pp. 477-491.

Alcântara Pereira, L.A., Ricci, J.E.R., Hirata, M.H. and Silveira-Neto, A., 2002, "Simulation of Vortex-Shedding Flow about a Circular Cylinder with Turbulence Modeling", Intern'l Society of CFD, Vol. 11, No. 3, October, pp. 315-322.

Arie, M., Kiya, M., Moriya, M. and Mori, H., 1983, "Pressure Fluctuations on the Surface of Two Circular Cylinders in Tandem Arrangement", ASME J. Fluids Eng. 105, pp. 161-167.

Batchelor, G.K. , 1967, "An Introduction to Fluid Dynamics", Cambridge University Press, Cambridge, UK.

Bernard, P.S., 1996, "A Vortex Method for Wall Bounded Turbulent Flows", ESAIM Proc., Vol. 1, 15.

Biermann, D. and Herrnstein, Jr., 1933, "The Interference between Struts in Various Combinations", National Advisory Committee for Aeronautics, Thecnical Report 468.

Chorin, A.J., 1993a, "Hairpin Removal in Vortex Interactions, II", J. Comp. Phys., Vol. 107, 1.

Chorin, A.J., 1993b, "Vorticity and Turbulence", Springer-Verlag, New York / Berlin, 1.

Chorin, A.J., 1973, "Numerical Study of Slightly Viscous Flow", Journal of Fluid Mechanics, Vol. 57, pp. 785-796.

Cotte, G.H., Michaux, B., Ossia, S, and VanderLinden, G., 2002, "A Comparison of Spectral and Vortex method in Three-Dimensional Incompressible Flows", J. Comp. Physics, 175, pp. 702-712.

Fernandez, V.M., Zabusky, N.J., Liu, P., Bhatt, S. and Gerasoulis, A., 1996, "Filament Surgey and Temporal Grid Adaptivity Extensions to a Parallel Tree Code for Simulation and Diagnosis in 3D Vortex Dynamics", ESAIM Proc., Vol. 1, 197.

Ferziger, J.H., 1981, "Numerical Methods for Engineering Application", John Wiley & Sons, Inc.

Fornberg, B., 1985, "Steady Viscous Flow Past a Circular Cylinder up to Reynolds number 600", Journal of Fluid Mechanics, Vol. 61, pp. 297-320.

Hiwada, M., Mabuchi, I. and Yanagihara, H., 1982, "Flow and Heat Transfer from Two same Size Circular Cylinders in Tandem Arrangement" (In Japanese), Trans. JSME 48, pp. 499-508.

Igarashi, T., 1984, "Characteristics of the Flow Around Two Circular Cylinders Arranged in Tandem", (Second Report), Bull. JSME 27 (233), pp. 2380-2387.

Igarashi, T., 1981, "Characteristics of the Flow Around Two Circular Cylinders Arranged in Tandem", (First Report), Bull. JSME 24 (188), pp. 323-331.

Jackson, C.P., 1987, "A Finite-Element Study of the Onset of Vortex Shedding in Flow Past Variously Shaped Bodies", Journal of Fluid Mechanics, Vol. 182, pp. 23-45.

Jendrzejczk, J.A. and Chen, S.S., 1986, "Fluid Forces on Two Circular Cylinders in Cross Flow", ASME, PVP 14, pp. 141-143.

Kamemoto, K., 2004, "On Contribution of Advanced Vortex Element Methods Toward Virtual Reality of Unsteady Vortical Flows in the New Generation of CFD", Proceedings of the 10th Brazilian Congress of Thermal Sciences and Engineering-ENCIT 2004, Rio de Janeiro, Brazil, Nov. 29 - Dec. 03, Invited Lecture-CIT04-IL04.

Kamemoto, K., 1993, "Procedure to Estimate Unstead Pressure Distribution for Vortex Method" (In Japanese), Trans. Jpn. Soc. Mech. Eng., Vol. 59, No. 568 B, pp. 3708-3713.

Kostic, Z.G. and Oka, .S.N, 1972, "Fluid Flow and Heat Transfer with Two Circular Cylinders in Cross Flow", Int. J. Heat Mass Transfer, 15, pp. 279-299.

Leonard, A. and Chua, K., 1989, "Three-Dimensional Interaction of Vortex Tubes", Physica D, vol. 37, pp. 490-496.

Lesieur, M. and Métais, O., 1996, "Spectral Large-Eddy Simulations of Isotropic and Stably-Stratified Turbulence", An. Rev. in Fluid Mech., Vol. 28, pp. 45-82.

Lewis, R.I., 1999, "Vortex Element Methods, the Most Natural Approach to Flow Simulation - A Review of Methodology with Applications", Proceedings of 1st Int. Conference on Vortex Methods, Kobe, Nov. 4-5, pp. 1-15.

Lewis, R. I., 1991, "Vortex Element Method for Fluid Dynamic Analysis of Engineering Systems", Cambridge Univ. Press, Cambridge, England, U.K..

Mansfield, J.R., Knio, O.M. and Meneveau, C., 1999, "Dynamic LES of Colliding Vortex Using a 3D Vortex Method", J. Comp. Phys., Vol. 152, pp. 305-345.

Mansfield, J.R., Knio, O.M. and Meneveau, C., 1998, "A Dynamics LES Scheme for the Vorticity Transport Equation: Formulation and a Priori Tests", J. Comp. Phys., vol. 145, pp. 693-730.

Métais, O. and Lesieur, M., 1992, "Spectral Large-Eddy Simulations of Isotropic and Stably-Stratified Turbulence", J. Fluid Mech., Vol. 239, pp. 157-194.

Mustto, A.A., Hirata, M.H. and Bodstein, G.C.R., 1998, "Discrete Vortex Method Simulation of the Flow Around a Circular Cylinder with and without Rotation", A.I.A.A. Paper 98-2409, Proceedings of the 16th A.I.A.A. Applied Aerodynamics Conference, Albuquerque, NM, USA, June.

Novak, J., 1974, "Strouhal Number of a Quadrangular Prism, Angle Iron and Two Circular Cylinders Arranged in Tandem", Acta Tech. CSAV 19 (3), pp. 361-373.

Ohya, Y., Okajima, A. and Hayashi, M., 1989, "Wake Interference and Vortex Shedding", In: Encyclopedia of Fluid Mechanics, Chap. 10 (Gulf Publishing, Houston, 1989).

Okajima, A., 1979, "Flow Around Two Tandem Circular Cylinders at very High Reynolds Numbers", Bull. JSME 22 (166), pp. 504-511.

Saghbine, J.C., 1996, "Simulation of Vorticity Dynamics in Swirling Flows, Mixing and Vortex Breakdown", M.Sc. Thesis, Department of Mechanical Engineering, Massachusetts Institute of Technology.

Sarpkaya, T., 1989, "Computational Methods with Vortices - The 1988 Freeman Scholar Lecture", Journal of Fluids Engineering, Vol. 111, pp. 5-52.

Sethian, J.I., 1991, "A Brief Overview of Vortex Method, Vortex Methods and Vortex Motion", SIAM. Philadelphia, pp. 1-32.

Shintani, M. and Akamatsu, T, 1994, "Investigation of Two Dimensional Discrete Vortex Method with Viscous Diffusion Model", Computational Fluid Dynamics Journal, Vol. 3, No. 2, pp. 237-254.

Smagorinsky, J., 1963, "General Circulation Experiments With the Primitive Equations", Mon. Weather Rev., Vol. 91, pp. 99-164.

Teixeira da Silveira, L., Alcântara Pereira, L.A. and Hirata, M.H., 2005, "The Effects of Interference between Two Circular Cylinders Arranged in Tandem by Vortex Method", 18th International Congress of Mechanical Engineering, Proceedings of COBEM 2005, November 6-11, Ouro Preto, MG.

Uhlman, J.S., 1992, "An Integral Equation Formulation of the Equation of an Incompressible Fluid", Naval Undersea Warfare Center, T.R. 10-086.

Zdravkovich, M.M., 1977, "Review of Flow Interference between Two Circular Cylinders in Various Arrangements", Trans. SAME, J. Fluid. Eng., 99, pp. 618-633.

Zdravkovich, M.M. and Pridden, D.L., 1977, "Interference between Two Circular Cylinders; Series of Unexpected Discontinuites", J. Ind. Aerodyn. 2, pp. 255-270.

Zdravkovich, M.M. and Pridden, D.L., 1975, "Flow Around Two Circular Cylinders", Research Report, Proceedings of the Second US National Conference on Wind Engineering Research, Fort Collins, IV (18).